

Memories of migrations past: Sociality and cognition in dynamic, seasonal environments

Eliezer Gurarie^{1,2,*}, Sriya Potluri¹, G. Christopher Cosner³, R. Stephen Cantrell³, William F. Fagan¹

¹*Department of Biology, University of Maryland, College Park, MD 20742, USA.*

²*Department of Environmental and Forest Biology, Syracuse, NY*

³*Department of Mathematics, The University of Miami, Coral Gables, FL 33146, USA.*

Correspondence*:
Eliezer Gurarie
egurarie@umd.edu

2 ABSTRACT

3 Seasonal migrations are a widespread and broadly successful strategy for animals to exploit

4 **Keywords:** keyword, keyword, keyword, keyword, keyword, keyword, keyword, keyword

1 INTRODUCTION

5 Seasonal migrations are widespread among terrestrial, aquatic, avian and invertebrate species
6 ([Dingle, 2014](#)). For many species, migration is an extremely successful strategy, allowing a far greater
7 number of individuals to inhabit landscapes which might not otherwise be able to support large
8 numbers year round ([Fryxell et al., 1988](#)). Essentially, the evolutionary stability of a migratory
9 strategy relies on the fitness benefits of accessing suitable seasonal resources, whether those are
10 for energetic gain, predator avoidance, or a suitable physical, biotic or social environment for
11 reproduction outweighing the energetic and survival related costs of migration ([Avgar et al., 2014](#)).

12 Proximate causes, drivers and mechanism can vary considerably across and even within species
13 ([Berthold, 1999](#); [Shaw, 2016](#)). Some migrants follow a “green wave” of spring vegetation as it
14 flowers across altitudinal or latitudinal gradients ([Bischof et al., 2012](#); [Kölzsch et al., 2015](#); [Merkle
15 et al., 2016](#)). These migrations can be considered “tactical”, as they can occur - as an extreme
16 simplification - purely as response to local conditions. Other migrants perform long-distance
17 migrations in anticipation that critical resources will be available at the time of arrival at the end
18 point of migration ([Abrahms et al., 2019](#)). This second behavior involves the greatest trade-off
19 between the costs of migration against the benefits of accessing resources, whether those are food,
20 suitable habitat for breeding, or refuge from predators, that are highly seasonal and localized. This
21 approach can be considered “strategic” in the sense that it is driven not by immediate cues but
22 by an anticipation based on prior experience ([Bracis and Mueller, 2017](#); [Merkle et al., 2019](#); [Bauer
23 et al., 2020](#)).

24 Migratory species may be more vulnerable to environmental change as disruption in either of the
25 seasonal ranges or along a migratory corridor can have significant negative impacts ([Wilcove and
26 Wikelski, 2008](#); [Seebacher and Post, 2015](#); [Kauffman et al., 2021](#)). On the other hand, migratory

species might be more resilient to large-scale disruptions due to their wide-ranging mobility (Robinson et al., 2009), and the cognitive and social factors determining the resilience of migrations to climate change are generally unknown. A long-distance migration can not rely entirely on local cues, and is therefore only possible if the behavior is hard-programmed or remembered. On the other hand, a strictly programmed behavior can be maladaptive if conditions change. While migration can clearly be a highly successful strategy, the resilience of migratory populations and migratory behavior is an open question and depends on the plasticity and adaptability of a population (Xu et al., 2021). That plasticity can take multiple forms, reflecting variation in *where*, *when* and *whether* the migration occurs Gurarie et al. (2017); Xu et al. (2021).

Cognitive processes, in particular spatial memory, have been shown and argued to be important mechanisms for the reinforcement and maintenance of migration (Merkle et al., 2019; Bauer et al., 2020). Similarly, sociality and social learning are likely essential to maintaining migration (Fagan et al., 2011; Jesmer et al., 2018; Berdahl et al., 2018). However, the interacting role of sociality and spatial memory for the plasticity of migration and the resilience of the behavior when faced with a changing environment is largely unstudied. Because the scenarios underlying migration are manifold and complex, mathematical modeling may provide some insights and help clarify where, when, and under what conditions we might expect migration behavior to emerge, to be adaptive, to be maladaptive, or to collapse.

Here, we develop a diffusion-advection model with sociality and memory to explore the resilience of a migratory population under various dynamic, seasonal resource distributions. In formulating the model, our goal was to identify the minimum set of movement and memory parameters required to generate an adaptive, migratory behavior. This includes the ability to learn to migrate from non-migratory initial conditions, simulating the release of naive animals in a seasonal environment (Jesmer et al., 2018), to lose the propensity to migrate if the resource distribution does not require it, also a commonly observed phenomenon (Wilcove and Wikelski, 2008), and to assess the resilience or fragility of a migratory population against changing resource distribution dynamics, including both stochasticity and trends in spatial and temporal distributions, mirroring the effects of climate change (Park et al., 2020).

We anticipated that under many conditions a blending of *tactical* (i.e. direct response to resource availability or perception) and *strategic* (i.e. memory-driven and forward-thinking) behavior will help foragers navigate dynamic, seasonal environments. Over-reliance on either strategy should be maladaptive. We further anticipate that a shorter-term memory updating is needed to navigate trends in resource spatial distribution and temporal distribution (phenology), but that a longer-term reference memory is needed to navigate resource distributions that are stochastic (Lin et al., 2021). Similarly, we anticipated that a balance between very low sociality and extreme sociality would lead to the most resilient migratory process.

2 METHODS

2.1 Memory movement model

In designing our study, our goal was to develop a minimal heuristic in which the following processes were explicitly modeled: (1) Random or exploratory movement, (2) attraction to resources, (3) a long-term (or *reference*) memory of large-scale movement behavior, (4) a short-term (or *working*) memory that updates movement behavior based on recent experience, and (5) some social aspect to the learned behavior.

A diffusion-advection equation provided a computationally efficient and versatile framework for examining just such a system. We consider a population moving in one dimension in a constrained domain D and distributing itself according to the following equation:

$$\frac{\partial u}{\partial t} = -\varepsilon \frac{\partial^2 u}{\partial x^2} + \alpha \frac{\partial}{\partial x} \left(u \frac{\partial h}{\partial x} \right) + \beta \frac{\partial}{\partial x} (v_s(u)) + v_m(t) \quad (1)$$

where u represents the population distributed in time and space. The first term is the diffusion term, capturing the fast time-scale exploration and “random” movements of individuals, with ε is the diffusion rate.

The second term represents the attraction to a dynamic resource h , with the proportionality of the advection to the gradient of the resource given by the parameter α (note, the population and resource distributions are functions of both space and time $u(x, t)$ and $h(x, t)$ - we omit the dependent variables in the notation for brevity). This is the well-studied standard chemotactic resource-following behavior. We borrow the general notation from our earlier related work (Fagan et al., 2017, 2019).

The third term captures the collective or social advection term of the population via a non-local, density dependent function $v_s(u, x)$. If this function takes the form of a convolution around a non-local kernel k , i.e. $v_s(u) = k(x) * u(x)$, and if that kernel is odd, an attractive or “swarming” behavior can be generated (Mogilner and Edelstein-Keshet, 1999). We use the kernel analyzed by Mogilner and Edelstein-Keshet (1999): $k(x) = \frac{x}{2\lambda^2} \exp(-x^2/2\lambda^2)$. The convolution of u with this kernel has the property of pushing the population in a positive direction when $x < \hat{u}$, and in a negative direction when $x > \hat{u}$. The parameter λ is a length scale of sociality - roughly one-half the size of the “swarm”, where β is a parameter that quantifies the overall strength of sociality.

Finally, the last term captures the direct advection that emerges from a memory-driven migratory behavior. This term evolves with a set of parameters θ_y that slowly change each year $y \in \{0, 1, 2, \dots\}$, i.e. the count of periods τ : $y = \lfloor t/\tau \rfloor$.

The migration speed is specified by six parameters θ : the timing of the start and duration of two anticipated seasons (nominally, winter and summer) t_1 , Δt_1 , t_2 , Δt_2 , and the spatial coordinates of the population centroid for each season x_1 and x_2 . Thus the remembered migratory speed term is a simple step function given by:

$$v_m(t, \theta_y) = \begin{cases} 0; & t > t_1 \text{ and } t \leq t_1 + \Delta t_1 \\ s_{12}; & t > t_1 + \Delta t_1 \text{ and } t \leq t_2 \\ 0; & t > t_2 \text{ and } t \leq t_2 + \Delta t_2 \\ s_{21}; & t > t_2 + \Delta t_2 \text{ or } t \leq t_1 \end{cases} \quad (2)$$

where the migration speeds s_{12} and s_{21} from the respective ranges are set such that they arrive at x_1 at t_1 , leave at $t = t_1 + \Delta t_1$, arrive at x_2 at $t = t_2$, i.e. $s_{12} = \frac{x_2 - x_1}{t_2 - (t_1 + \Delta t_1)}$ and $s_{21} = \frac{x_1 - x_2}{t_1 - (t_2 - \tau + \Delta t_2)}$. This step-like migration function is a one-dimensional version of the migration parameters estimated in empirical studies for individuals (Gurarie et al., 2017) and, more relevantly, for populations (Gurarie et al., 2019) in empirical studies.

We consider these six parameters to be the known or remembered determinants of the migratory behavior, with an initial set θ_0 determining the reference migration behavior. This reference migration is updated each year by the experience of the population. To perform this updating, we estimate a new set of parameters $\widehat{\theta}_y$ after each year, and combine these new parameters with the reference parameters according to the following weighted mean:

$$\theta_{y+1} = \kappa^y \theta_0 + (1 - \kappa^y) \widehat{\theta}_y$$

where each of the six parameters is updated identically. The estimates $\widehat{\theta}_y$ are obtained via a least-squares minimization of the migration track ($m(t, \theta) = \int_0^t v_m(t', \theta_y) \Delta t'$) against the spatial mean of the population process in year y (i.e. $\widehat{u}(t) = \int_X u_y(t, x) dx$). The parameter $\kappa \in (0, 1)$ captures the reliance on that long-term memory. When $\kappa = 0$, all of the actionable memory is from the preceding year. When $\kappa = 1$, the actionable memory is entirely the reference memory.

The model is confined to a one-dimensional bounded domain $[-\chi, \chi]$, with no flux outside of the boundaries i.e. $\partial u(-\chi, t)/\partial t = \partial u(\chi, t)/\partial t = 0$. As there are no birth or death processes, the total population remains fixed and constant, for convenience integrating to 1. Furthermore, the parameters remain constant throughout time, with no adaptation or mutation-selection process. Our interest is entirely in the ability of a fixed set of memory and movement parameters to navigate an intra- and interannually dynamic, seasonal environment.

2.2 Seasonal resource

We solved the model numerically on a spatial domain $x \in [-100, 100]$, and a periodicity $\tau = 100$ (i.e. ~years of 100 days). We were interested in an approximately periodic resource dynamic, i.e. one in which $h(x, t \approx h(x, t - \tau))$. We generated two types of resource distributions. A “non-surfable” resource (*island resource*), and weakly surfable resource (*drifting resource*). Both are characterized by a peak in time and space centered at m_x at m_t , and $-m_x$ at $\tau - m_t$ (for example, locations 30 and -30 at times 25 and 75, respectively). These pulses have a shared time scale of duration s_t and a spatial scale of extent s_x , the standard deviation in the time and space dimension respectively. The island resource is simply two uncorrelated bivariate normal distributions

$$h(x, t) = K (\Phi(m_x, m_t, s_x, s_t) + \Phi(-m_x, \tau - m_t, s_x, s_t))$$

where Φ is the bivariate Gaussian distribution function, and the normalizing constant K is selected such that the average total amount of resource throughout the year is 1, i.e. $\frac{1}{\tau} \int_T \int_X h(x, t) dx dt = 1$.

The drifting resource differs from the island resource in that the total amount of resource at any given time $\int_X h(x, t) dx = 1$. This property is attained by distributing the resource as a re-scaled beta distribution, where the shape and scale parameters vary sinusoidally in such a way as to make the standard deviations and means match the desired values of m_x, m_t, s_x, s_t (see Supplementary Materials for details). Both types of resources are illustrated in figure 1.

Within a given year, the resource is entirely symmetric: $h_y(x, t) = h_y(-x, \tau - t)$. However, in scenarios exploring climate change we allow the peaks to vary with drift and stochasticity according to: $m_x(y) \sim N(\mu_x + \gamma_x y, \sigma_x)$ and $m_t(y) \sim N(\mu_t + \gamma_t y, \sigma_t)$, where the μ , γ and σ terms are the mean, slope and variance, respectively, for the location and time duration of the pulse. Thus, if $\gamma = 0$ and $\sigma = 0$, the conditions are constant across years and if $\gamma_x > 0$ there is a drift of the resource towards extremes, if $\beta_t < 0$ there is a shift towards earlier resource pulses. These trends model the

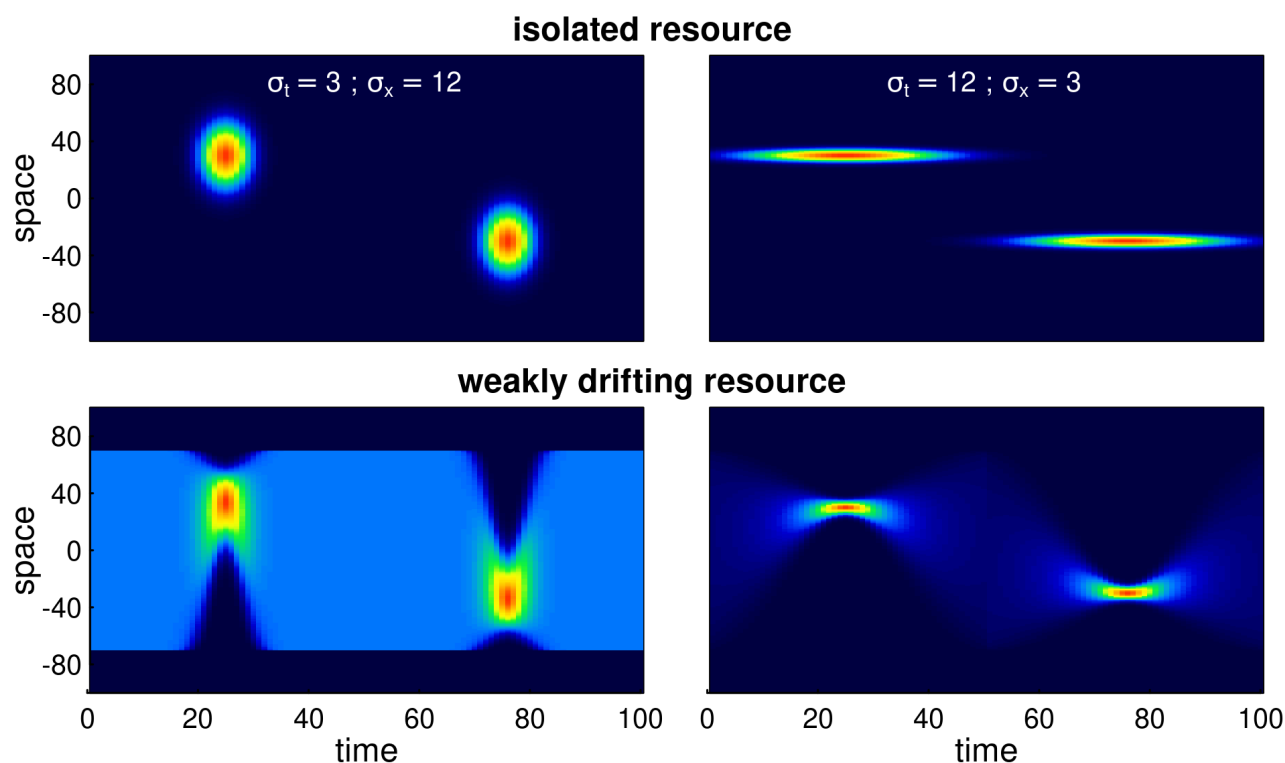


Figure 1. Examples of various seasonal resource distribution functions, contrasting short duration, but wide pulses ($\sigma_t = 3, \sigma_x = 12$; left panels), long duration but spatially concentrated pulses ($\sigma_t = 12, \sigma_x = 3$; right panels), and isolated resource pulses (upper panels) from the weakly drifting resource (lower panels). The total amount of resource is identical across all scenarios. In the weakly drifting resources, the total amount is constant at all times, and uniform in the middle of the phase (time = 0, 50, 100).

131 pole-ward shift of peak resources and the earlier spring phenology occurring with a warming global
 132 climate. The spatial scales (s_x and s_t) remain constant in all of our simulations.

133 2.3 Metrics

134 The main metrics we are interested in are *migration mismatch*, *foraging efficiency* and *adaptation*
 135 *to trends*.

136 Migration mismatch captures the similarity between the migration phenology and the resource
 137 phenology. To do this, we compute the total mismatch, i.e. is a sum of the difference between
 138 the migration coefficients and the resource peaks. Spatial mismatch MM_x is given by the absolute
 139 difference between the migration targets and the resource peaks: $MM_x = |x_1 - m_x| + |x_2 + m_x|$.
 140 Temporal mismatch is the difference between the arrival time and the peak of the resource if
 141 arrival is post-peak, the difference between the departure time and the peak of the resource if
 142 departure is pre-peak, and 0 if the seasonal duration spans the peak, i.e. $MM_t = \max\{t_1 - m_1, m_1 -$
 143 $(t_1 + \Delta t_1), 0\} + \max\{t_2 - m_2, m_2 - (t_2 + \Delta t_2), 0\}$. Finally, the total mismatch is the sum of these:
 144 $TM = MM_x + MM_t$. A mismatch of less than 1 is essentially perfect, we consider a mismatch of 1-5
 145 to be “good”, and beyond 50 the system can be said to have failed to keep track of the resource
 146 dynamics.

To quantify the foraging efficiency, i.e. the organisms' ability to track the distribution of the resources over space and time, we use a continuous form of the Bhattacharyya coefficient (Bhattacharyya, 1943) which quantifies the similarity between two distributions. We compute this coefficient at every time point in a given year, and take the mean across the equilibrium year to determine foraging efficiency (FE). Thus, the foraging efficiency index is:

$$FE = \frac{1}{\tau} \int_0^\tau \int_{-\chi}^\chi \sqrt{u(x, t) h(x, t)} dx dt$$

where the spatial integral is taken over the domain. This metric is constrained to be between 0 and 1.

For simulations with a constant resource, we ran the model until a quasi-equilibrium (stationary) state was achieved, i.e. where the Bhattacharyya index of the population distribution across subsequent years reached a value of 0.9999. Once stationarity was attained, we computed the migration mismatch and foraging efficiency metrics, as well as the number of years required to reach stationarity.

For numerical runs with climate change, we first run a simulation with a given parameter set until stationarity, as above, and then begin shifting the location of the resource poleward with a slow, moderate or rapid trend ($\gamma_x = 0.25, 0.5$ and 1 , respectively), and / or by adding stochasticity (spatial standard deviation 3, 6, 9 or 12). For stochasticity analyses, we compare foraging efficiency across a range of the reference memory parameter κ . For analyses that include trend (with or without stochasticity), we quantified the ability of the system to keep track of climate change with a *spatial adaptation* (SA) index. This index is the ratio of the slope of the memory-based migration location over time (i.e. the fitted slope coefficient of $m_{x,i} = \hat{\gamma}_x i + m_{x,0}$, where i is the year) against the resource drift parameter γ_x , i.e. $SA = \hat{\gamma} / \gamma_x$. An SA equal to 1 suggests that the process is keeping up with climate change, an SA of 0 indicates that the process is not responding at all to climate change. Values greater than 1 (super-adaptation) are possible, as are values less than 1, which correspond to a loss of migration behavior.

All movement model parameters, resource parameters, and metrics are summarized in table 1.

2.4 Simulation studies

We explored this model using numerical differencing of a system of ordinary differential equations (ODE's) approximating the PDE in equation 1 with the Runge-Kutte algorithm using the `deSolve` (Soetaert et al., 2010) and `ReacTran` (Soetaert and Meysman, 2012) packages in R. We additionally used the `nlsLM` function in package `minpack.LM` (Elzhov et al., 2016) for robust and fast annual estimation of the migration parameters. The complete code is available as an R package (`memorymigration`) available on GitHub at <https://github.com/EliGurarie/memorymigration> and as an interactive Shiny application at <https://spot3512.shinyapps.io/memorymigrationshinyapp/>.

We assessed a wide range of parameter values and resource geometries and dynamics with the goal of answering the four main questions: (1) Can this model adapt to a discrete shift in peak resource location and timing? What is the relative role of memory and sociality for adaptation? (2) Can this model acquire a migratory behavior from a non-migratory initial condition? (3) What is the role of a reference memory for dealing with stochastic resource dynamics? (4) Can this model adapt when the resource peaks shifts in space?

3 RESULTS

3.1 Adaptation to resource phenology

The ability of this system to attain a stable, migratory state that matches the dynamics of the resource is illustrated in figure 2. In the illustrated scenario, it takes nearly 40 years to attain an equilibrium, and the eventual steady state is one where the centroid of the migration lines up exactly with the centroid of the resource, and the arrival timing coincides with the peak of resource availability. Notably, the path to this equilibrium is somewhat indirect, with the later winter range taking more time to stabilize than the earlier summer range. The eventual steady state is one where the foraging efficiency is relatively high.

We ran this process for 8100 parameter combinations (figure 3). The fundamental dynamic of attaining and maintaining a well-matched migration phenology, can occur under many combinations of parameter values, but all parameters play a role. Among the more intuitive results are that greater values of α (resource following) lead to an improved ability to match the migration. Resource peaks with larger spatial extent (higher σ_x) are generally better for migration matching. A larger set of parameters matched migration with low diffusion than high diffusion.

Less intuitive was the high importance of the sociality parameters, in particular the spatial scale of the swarming. Higher levels of social attraction (β) led to improved migration matching except in those cases where the sociality scale λ was high. Thus, for example, at $\lambda = 20$, no simulations at $\beta \geq 200$ managed to acquire or maintain a matched migration. However, at $\lambda = 50$ or 100, the migration was slightly better matched at high values of β (figure 3). The spatial extent of the swarm

Table 1. Table of parameters, variables and metrics.

Memory migration model	
ϵ	Diffusion
α	Forage following
β	Strength of sociality
λ	Spatial scale of sociality
κ	Proportion of reference versus working memory
x_1, x_2	location of population centroids in summer and winter
$t_1, \Delta t_1$	start and duration of summer season
$t_2, \Delta t_2$	start and duration of winter season
κ	proportion memory allocated to reference (long-term) memory vs. working (short-term) memory
Resource dynamics	
τ	duration of period (year)
$m_x, -m_x$	spatial coordinate of resource peak for summer and winter
$m_t, \tau - m_t$	timing of resource peak for the summer and winter
σ_x, σ_t	time duration and and spatial scale of resource pulse
γ_x, γ_t	rate of change of peak location and timing of resource
ψ_x, ψ_t	standard deviation of peak location and timing
Metrics	
MM_x	spatial migration mismatch
MM_t	temporal migration mismatch
TM	total mismatch
FE	foraging efficiency
SA	spatial adaptation index

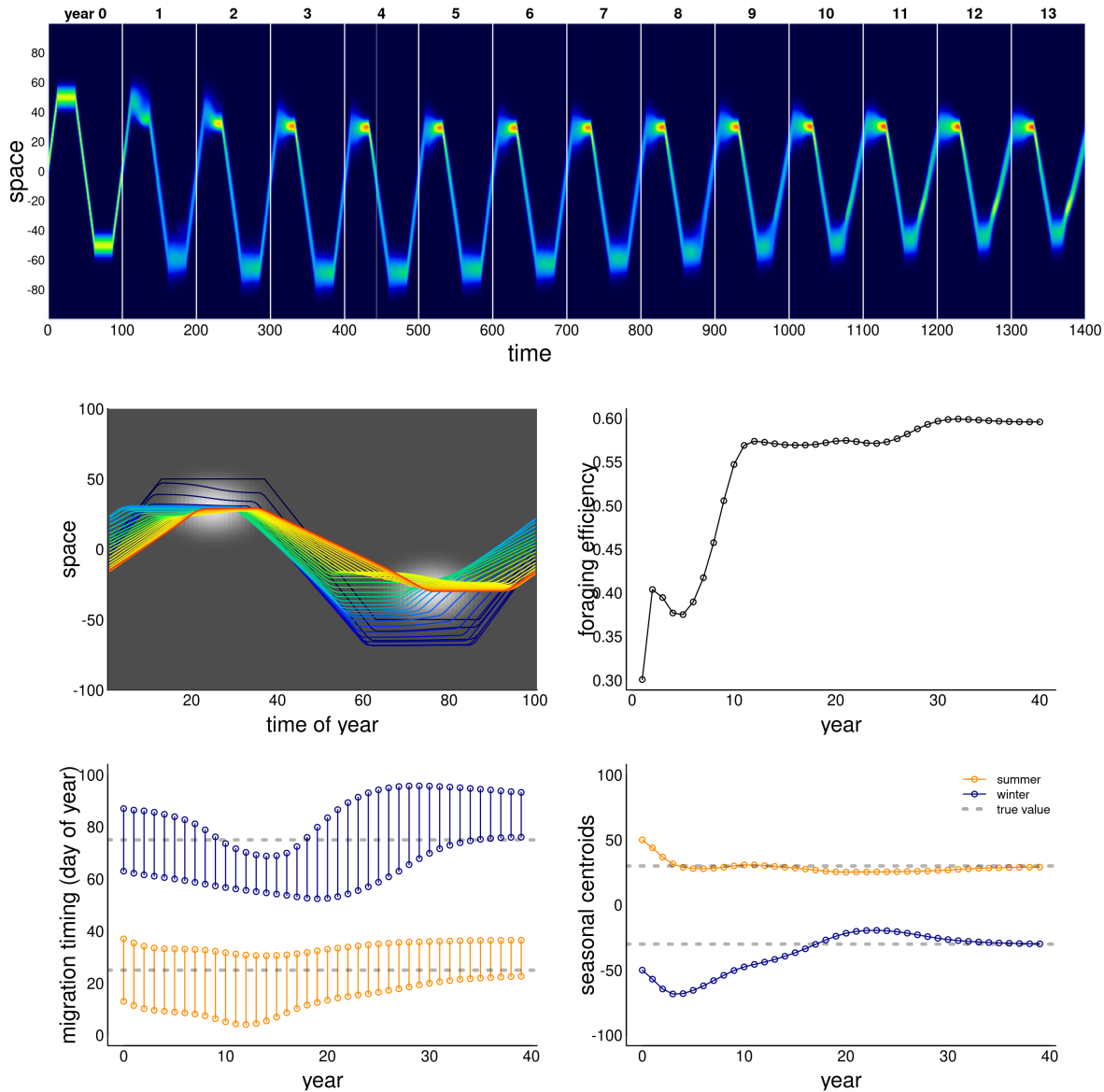


Figure 2. Example of adaptation to a shift in resource peak. The initial (year 0) behavior migrates to locations 50 and -50 at days 15 and 60, whereas the resource peak is at 30 and -30, peaking at times 25 and 75. The panels show (a) the first 14 years of the simulation; (b) the centroid of the annual movement of the population is shown in panel b, with dark blue to red colors indicating year 0 to year 40; (c) annual foraging efficiency across years; (d) migration timing parameters for each year, with orange segments indicating arrival and departure from the summering (northern) grounds, and the blue segments indicating timing of arrival and departure at the wintering grounds; (e) migration arrival and departure location across years, with blue and orange indicating winter (southern) and summer (northern) locations.

was a remarkably significant variable. Smaller swarms were able to match migration only at low values of social attraction ($\beta = 200$), and relatively high values of resource attraction ($\alpha \geq 600$).

Random forest analyses, whether on the log of total mismatch or on the classification of a perfect match, uniformly show that the most important variables (Breiman, 2001) were α and λ (4.14 and

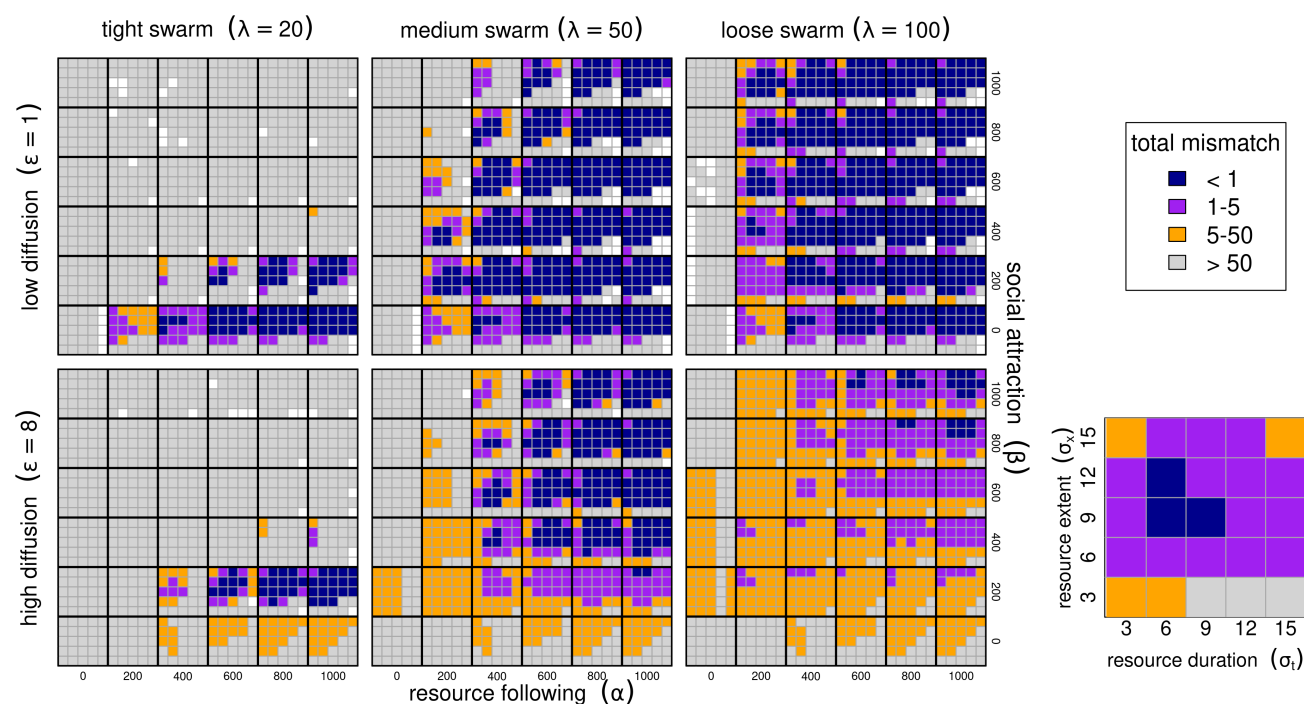


Figure 3. Migration phenology matching across six model parameters. Low and high diffusion ($\epsilon = 1$ and 8 in upper and lower panel blocks), tight, medium and loose swarms ($\lambda = 20, 50, 100$) left to right panels. Within each of these blocks, high values of the resource following parameters α from 0 to 1000 are left to right, and higher values of the sociality parameter β are bottom to top. Within each of the combinations of $\epsilon, \lambda, \alpha, \beta$, we show results ranging across 6 values of resource duration (σ_t , 3 to 15 left to right), and 6 values of resource extent (σ_x , 3 to 15 bottom to top), as in the zoomed-in panel at (bottom right). The color scheme reflects the total mismatch, i.e. the sum of the absolute differences between the migration timing and locations from the resource peak. White squares represent runs that numerically failed to estimate migration parameters.

204 4.02 proportional increase in MSE), and the least important was σ_t , with a 0.5 proportional increase
 205 (table X).

206 Overall, foraging efficiency was strongly correlated with migration matching, as expected. At high
 207 mismatch (> 50), foraging efficiency was low (mean 0.29, s.d. 0.16) compared to the near-perfect
 208 matching migrations (mean 0.58, s.d. 0.14). However, somewhat higher mismatch (1 to 5) showed
 209 an even higher overall foraging efficiency (mean 0.62, s.d. 0.18 - see also figure 4).

210 3.2 Learning to migrate

211 Figure 5 illustrates the ability of the model animals to learn to migrate in a weakly drifting
 212 resource environment with a narrow pulse of resource peaking at 30 and -30 (at days 25 and 75), but
 213 a uniform distribution of resource at times 0 and 50. In order to learn to migrate, the system needed
 214 to have a higher exploratory impulse (higher diffusion constant ϵ), a stronger resource advection
 215 (higher α) and somewhat weaker sociality (lower β). The qualitative behavior of this process was
 216 to start drifting towards the summer resource, while slowly developing a weak pulse towards the
 217 winter resource as well. After first locking in on the summer resource, the winter migration, driven
 218 both by high diffusion and high resource following, slowly extended itself until both narrow peaks of
 219 resource can be consistently reached.

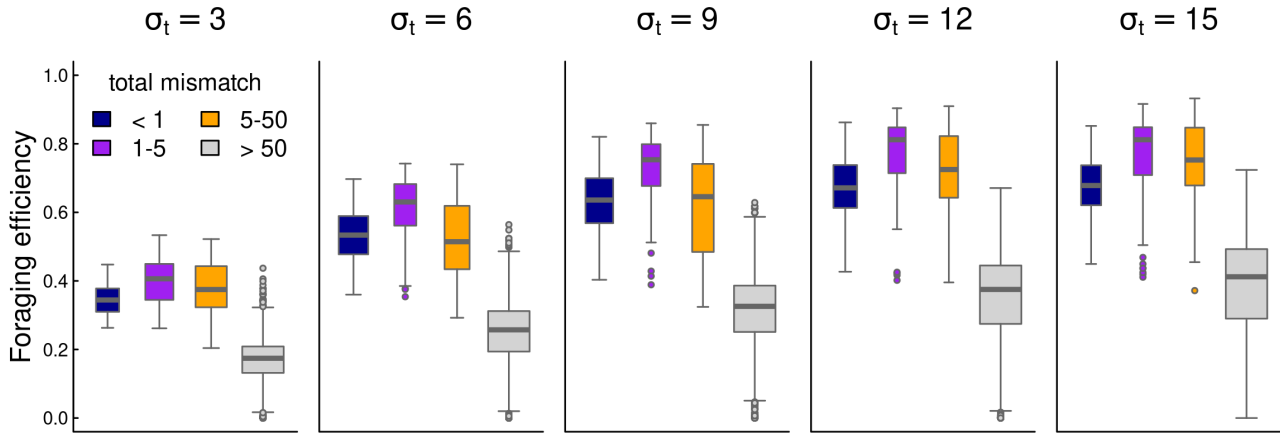


Figure 4. Box-plots of foraging efficiency against mismatch across several values of foraging patch duration.

220 The model had, in general, a difficult time learning migration from a non-migratory initial
 221 condition. Thus, out of 4047 successful runs, only 4 attained mismatch below 1, and 130 below 5.
 222 Conditions that were more conducive to learning migration were pulses of *longer* duration (high σ_t),
 223 but *smaller* in scope (low σ_x), suggesting that the feedback that encourages migration needs to be
 224 compact in space but long enough in duration to lock in to the memory.

225 3.3 Adapting to climate change

226 To assess the ability of the system to adapt to a trending climate, we generated scenarios with
 227 slow (0.25 units / year), medium (0.5 units / year), and fast (1 unit / year) drift outward of the
 228 two resource pulses. We then assessed 40 parameter combinations for each of those scenarios, a
 229 high and low value of resource following ($\alpha = 400$ and 100) crossed with a high and low value of
 230 sociality ($\beta = 400$ and 100) crossed with 10 values of the spatial scale of sociality ($\lambda = 20$ to 200).
 231 The spatial and temporal scale of the resource pulses were fixed to a relatively “easy” to adapt to
 232 $\sigma_x = 12$ and $\sigma_t = 6$. We computed the adaptation index and foraging efficiency for each of the 120
 233 runs (figure 6). We were interested in the dynamics against λ due to the uniformly high importance
 234 of this parameter for determining the success of this process to match migration in steady states.

235 As figure 6 shows, higher values of resource following ($\alpha = 400$; orange circles) are nearly universally
 236 better for keeping up with climate change (SA values near 1). Furthermore, when combined with
 237 high sociality ($\beta = 400$; right panels), nearly all parameter combinations do a good job keeping
 238 up with climate change (SA values ranging between 0.53 and 0.85 for a swarm size greater than
 239 50). However, that maximum value is still less than 1, suggesting that truly matching a steadily
 240 drifting trend is very difficult. Small swarms ($\lambda < 50$) have a very hard time adapting when the
 241 social attraction is high, but do fairly well when social attraction is lower. But larger sized swarms
 242 do progressively worse across more parameterizations, e.g. in the most rapid climate change scenario,
 243 the SA drops from 0.83 to -0.13 as the swarm increases in size from 40 to 200 (essentially, the entire
 244 spatial domain).

245 A rather more dramatic pattern is visible for the lower foraging attraction scenario ($\alpha = 100$; blue
 246 circles). Notably, no parameter combination at this value comes close to keeping up with the rapid
 247 climate change (SA range -0.64 to 0.13). For slower climate change, however, there is a window

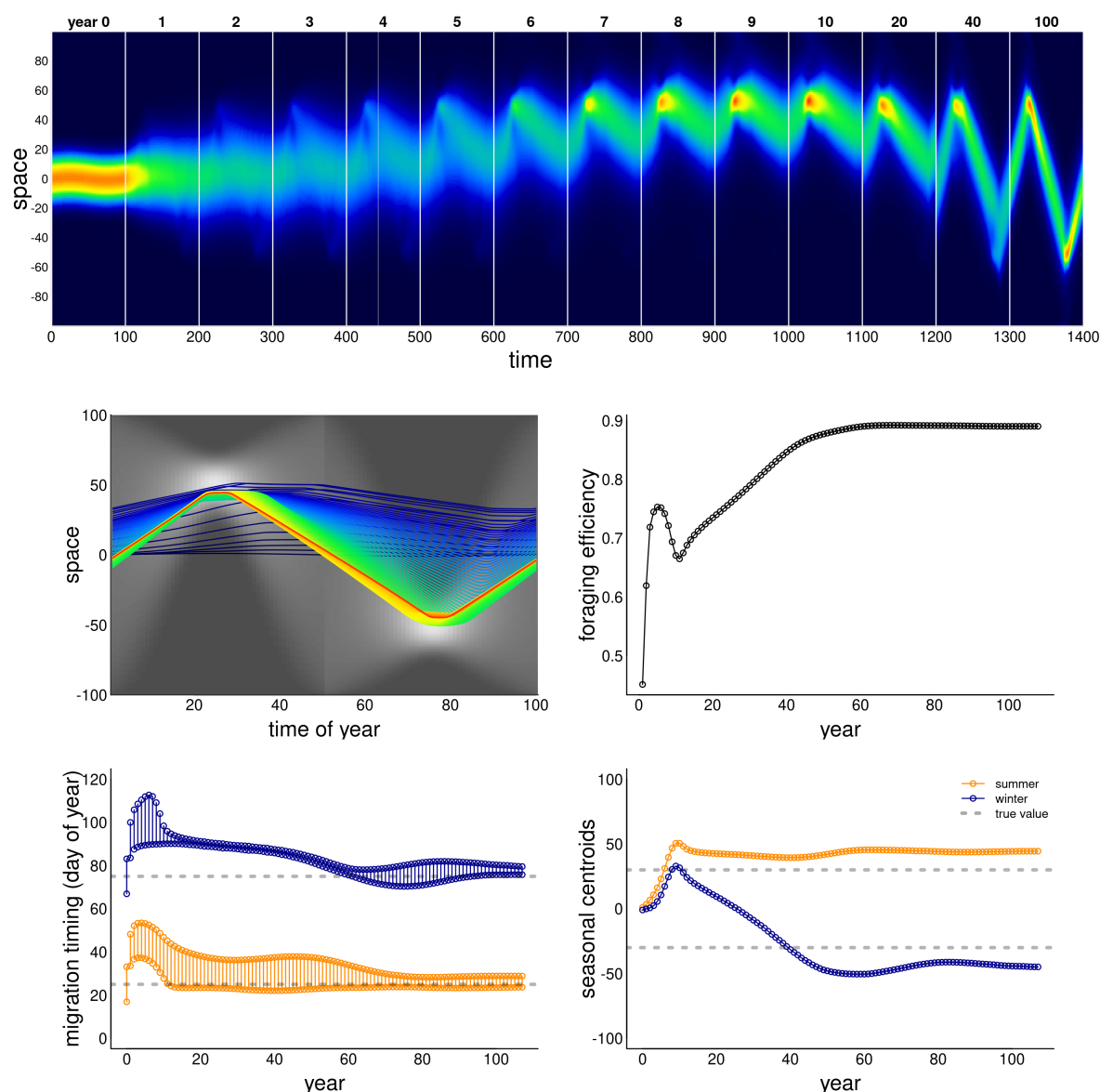


Figure 5. Example of model learning to migrate. The resource is a “weakly drifting” resource and the initial (year 0) condition is non-migratory. The simulation was run for 100 years, and a sampling of those years (labeled) are presented in panel a: all years from 0 to 10, followed by 20, 40 and 100. Otherwise, panels are as in figure 2. Additional parameter values were $\epsilon = 5$, $\alpha = 500$, $\beta = 50$ and $\lambda = 40$.

of values for the swarm size between 40 and 80, where the SA *exceeds* 1, and then crashing quite rapidly to negative values of SA as that swarm size increases. These “super-adaptive” processes indicate a unique sweet spot where a swarm is large enough to capture and adapt to the drifting resource, but not so large that the information gathered in a given year is too weak to adjust the migratory behavior in a following year.

As anticipated, better adaptation to the drifting resource correlated strongly with higher foraging efficiency (inset boxplots).

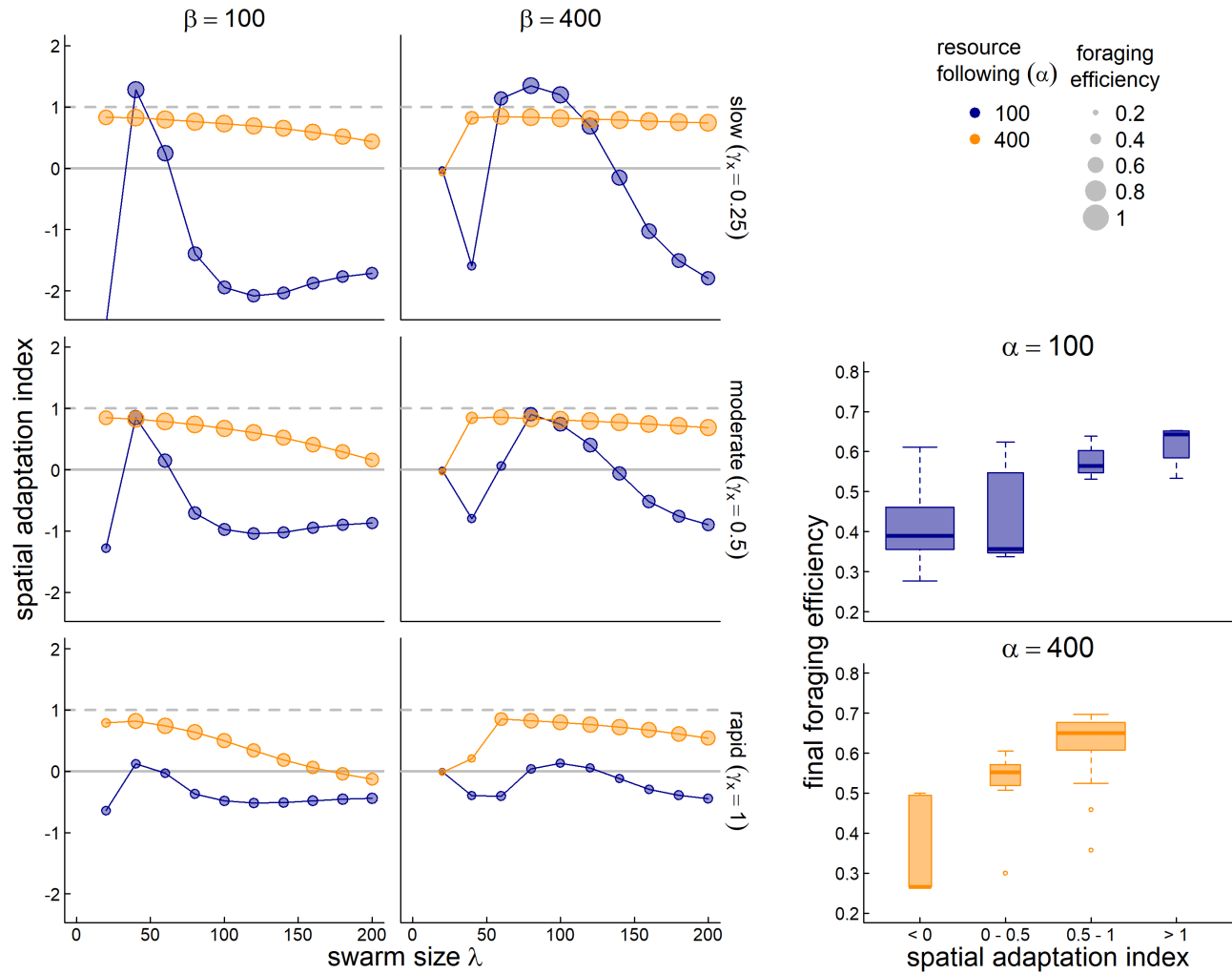


Figure 6. Adaptation to a steadily drifting resource. In three scenarios, the spatial coordinates of the resource drift by 0.25, 0.5, and 1 unit per year (top to bottom, respectively). The y-axis is the spatial adaptation index (SA), i.e. the trend of the memory-driven migration divided by the resource drift trend. Values near 1 indicate a behavior that keeps up with climate change, values near 0 indicate no change in migration behavior, and negative values indicate a trend that is opposite to the climate trend. We compare across spatial scales of sociality (λ - x-axis), for low and high values resource following ($\alpha = 400$ and 100 - orange and blue dots) and low and high values of sociality ($\beta = 100$ and 400 , left and right panels). The size of the circles is proportional to the foraging efficiency of the resulting parameter combinations. The bottom-right boxplots indicate the final year foraging efficiency against SA; purple and blue boxes indicate the highest values, orange and gray lower values.

255 3.4 Reference memory and stochasticity

256 While recent memory can be helpful for adapting to a single novelty or a smoothly changing
 257 conditions, we hypothesized that more conservative approach, relying on a “reference memory” may
 258 be more beneficial when conditions change stochastically. We tested this hypothesis by solving a
 259 set of models across a range of κ values from 0 (all recent memory) to 1 (all reference memory). In
 260 these scenarios, we ran the system for as many years as needed with no stochasticity to acquire
 261 a stationary state (i.e. similarity index greater than $1\text{-}1\text{e-}6$). We then used the stationary state

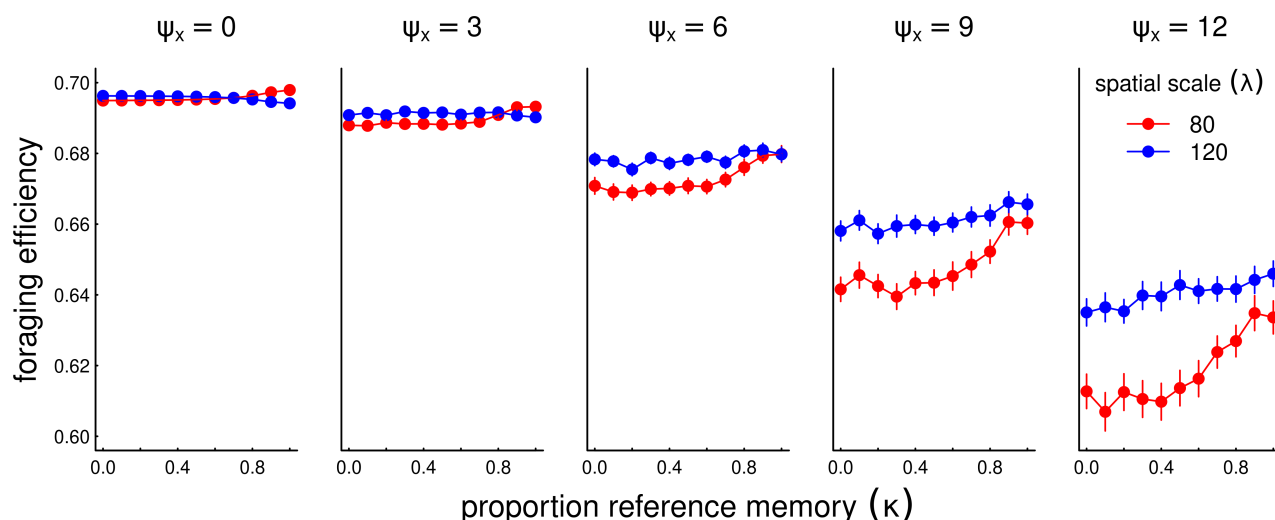


Figure 7. Foraging efficiency (FE) across various values of reference memory κ (x-axis) for increasing amounts of interannual stochasticity (ψ_x , panels left to right), and two values of sociality spatial scale $\lambda = 80$ and 120. For the processes with non-zero stochasticity ($\psi_x > 0$), the process was run 90 times for values of κ . Points represent the average of the FE's across all 50 years and 90 replicates, and shaded areas represent a local regression (loess) smooth of FE against κ . In these scenarios, the resource following parameter $\alpha = 100$, the social attraction $\beta = 400$ and diffusion $\epsilon = 4$.

as the reference memory, and then ran the process for an additional 50 years with a stochasticity (i.e. standard deviation in peak location of the resource) ranging from 0 to 12.

Figure 7 illustrates that, as predicted, the highest level of κ can significantly help foraging efficiency, with some variation across the spatial scale of sociality. When that scale of sociality is high enough (e.g. $\lambda = 120$, blue colors) there is greater probability of overlap with a stochastic resource, and a conservative, stable migratory regime is much more beneficial in the long run. Overall, as anticipated, the greater the stochasticity, the lower the foraging efficiency; and the greater the stochasticity, the greater the benefit of a conservative reference memory driven strategy.

3.5 Stochasticity and trends

We added trends to the stochastic process described above, adding 30 years of spatial outward trend in the resource. Our goal was to assess the ability of the process to keep up with climate change as a function of the reference memory parameter (figure 8). Over-reliance on reference memory ($\kappa = 1$) by definition does not allow the system to keep up with climate change, leading to an adaptation index of 0. However, in many cases a balancing of recent and reference memory (κ value between 0.6 and 0.8) in many cases was slightly but significantly better than relying entirely on recent memory. The smaller spatial scale (in the selected parameter space) does a generally better job than the larger spatial scale at lower stochasticity. At higher level of stochasticity, however, the larger spatial scale outperforms the smaller spatial scale, which completely loses track of the climate change.

4 DISCUSSION

Animals navigate complex, dynamic and patchy environments. When there is a strongly localized and seasonal component to the resource dynamics, movement strategies limited to straightforward resource-following taxis necessarily fail to maximally exploit the dynamics. It is in these cases, quite

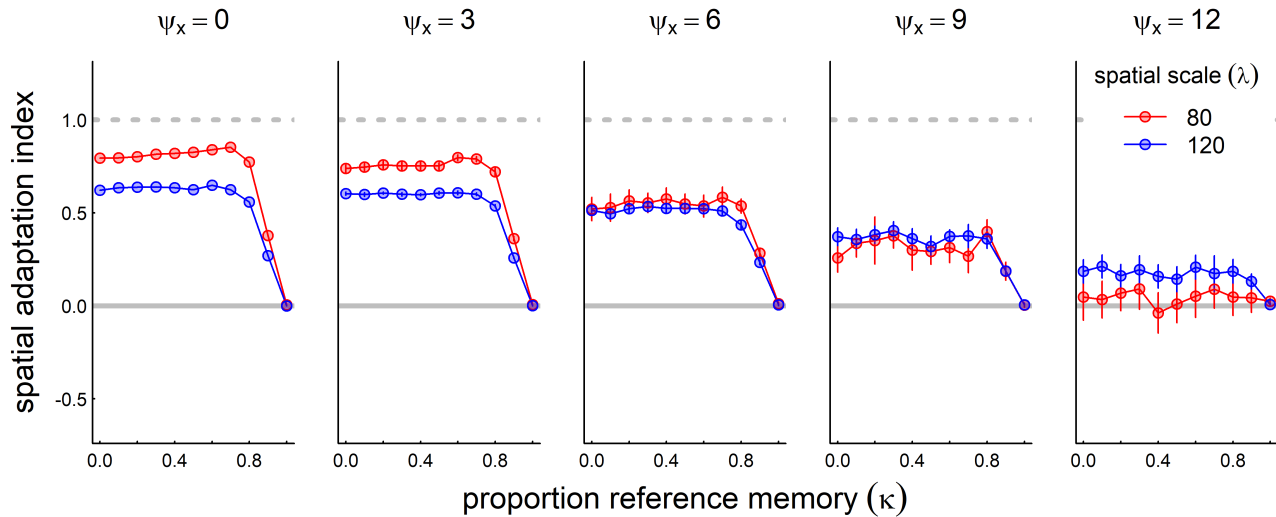


Figure 8. Role of reference memory in adapting to climate change for increasingly stochastic resource dynamics. We ran the model with a moderate rate of climate change (mean shift: 0.5/year) at five increasing levels of stochasticity (inter-annual standard deviation of resource peak 0, 3, 6 and 12, left to right panels). For non-zero stochasticity, we ran the process 30 times and present the mean and standard error of the spatial adaptation index across various values of the reference memory parameter κ : where $\kappa = 0$, the system modifies its migration based entirely on recent experiences; at $\kappa = 1$, the memory never changes from the reference memory. Other parameter values are resource following $\alpha = 100$, social attraction $\beta = 400$, and diffusion $\epsilon = 4$.

284 common in the natural world, that seasonal migration becomes a viable, even necessary, strategy.
 285 However, when resources start shifting in space and time – as is occurring at an accelerated pace
 286 with recent global climate change – the migration phenology itself must exhibit some plasticity.
 287 It is our conjecture that this plasticity is facilitated by a memory-driven process, in which recent
 288 experiences inform strategic behaviors in subsequent years, combined with a social dynamic. The
 289 relatively simple, social and memory-driven mechanism we propose here was, in fact, able to adapt
 290 to long-term changes in resource dynamics, even with inter-annual stochasticity. The model thereby
 291 provides a framework with which the interaction of memory, movement, social and resource dynamics
 292 can be explored.

293 We found that the straightforward inclusion of a migration-specific memory in a social diffusion-
 294 advection framework was sufficient to capture many fundamental phenomena related to migration.
 295 In essence, our model allowed a population with a hybrid migratory and resource-following behavior
 296 to adjust the migratory behavior based on recent experiences with the resource location. The model
 297 was able to emulate the successful navigation of an environment with temporally and spatially
 298 isolated seasonal resource patches, the spontaneous emergence of a migratory behavior, and intrinsic
 299 robustness to changes in those environmental resources, whether those changes were steadily shifting
 300 trends or inter-annual stochasticity. In a generalized way, it captured all three fundamental types of
 301 migration plasticity: the *where*, the *when* and the *whether* (Xu et al., 2021).

302 Our goal was to understand the combinations of factors that lead to a resilient migration behavior.
 303 We used foraging efficiency as a convenient metric of the utility of migration, but this was not a
 304 measure explicitly maximized by the model. Other metrics, such as foraging efficiency in a given
 305 season, or probability of survival or reproduction relative to resource availability (Bauer et al.,

2020) may respond differently across model parameters and could be useful in understanding the relative success of alternative migratory strategies in different contexts. However, the overall annually averaged metric provided the broadest linkage between resource dynamics and animals' locations and was consistent with the minimal biological assumptions and generality of our framework.

Among the general conclusions from our model, one is that migration can be acquired in a seasonal environment, even with no strong intrinsic propensity to migrate and a weak phenological resource pulse to follow. This has been demonstrated for translocated ungulates (Jesmer et al., 2018), even in environments where resources are difficult to “surf” (figure 5). Learning migration, however, requires a very strong resource attraction, higher levels of exploratory behavior (e.g. diffusion, and larger spatial scale of sociality), and – often — many more years. These findings echo empirical observations (Jesmer et al., 2018). On the other hand, migrations can be considered somewhat fragile, in the sense that under certain conditions, e.g. increasing stochasticity, rapidly shifting resources, a shift in some of the system parameters, or even a shift in the spatial and temporal extent of resources, migration can collapse and turn into a non-migratory, residential behavior (figure 3). This sensitivity may explain why partially migratory populations composed of a mixture of resident and migratory individuals are so common and, apparently, evolutionarily stable (Berthold, 1999; Chapman et al., 2011), as well as the wide range of migration plasticity shown in wild populations, even within a species (Xu et al., 2021).

The ability to maintain, learn and adapt a migration also depends strongly on properties of the resource dynamics. In particular, the reinforcement of memory and foraging is strongest when patches are concentrated in time, but relatively large in space. Interestingly, in most stable patterns, the eventual targeted migration arrival time coincided with the *peak*, rather than the beginning, of the resource dynamic. This indicates that the long-distance social migration behavior may be particularly reinforced when the targeted resource is very sudden. This is the case for the rapid green-up that occurs in high latitudes as snow recedes in tandem with extended day lengths leading to an intense green-up period (Park et al., 2020) or, for example, when resources are linked to the short-duration early blooming phenology of very particular plants (Renner and Zohner, 2018).

The sociality parameters – in particular, the spatial scale λ – were, unexpectedly, the most important parameters for determining the resiliency of the process. In particular, a population with a small spatial scale tended to have a much more difficult time locking in to an adaptive migratory pattern, and only in conditions where the social attraction was relatively weak. In order to adapt to any shift in resources, some individuals must experience that resource, and the two sociality-related mechanisms to have that scope are either a relatively large spatial scale or a relatively weak social cohesion. On the other hand, overly large spatial scales compromised the ability of the process to track climate change, due to a dilution of the population's ability to concentrate over available resource patches. Thus, there appear to be multiple avenues by which 'sociality' can structure migration. For example this could tie into the relative balance between individuals exploring the landscape to acquire new information about resources and their opportunities to interact with other individuals and communicate (or attract).

All of the parameters in our model have well-defined biological interpretations. The diffusion (ϵ) captures short time-scaled randomness of movement, capturing the exploratory and short-term dispersive behavior. The foraging advection strength (α) captures the attraction of the population to better quality resources at a relatively large scale. These two parameters, the basic ingredients in diffusion-advection models of animal movement, have direct parallels to empirically estimated

properties of animal behavior: diffusion is closely related to families of random walk models (Gurarie and Ovaskainen, 2011) while the advective taxis is related to the step- and resource selection functions that are routinely estimated from movement data (Potts and Schlägel, 2020). The spatial scale of the social group (λ) captures the spatial extent of the population, i.e. a population-level range. The sociality parameter (β) quantifies the strength an individual's desire to approach the center of the social group. This is not a parameter that is typically measured, though it would - in principle - be possible to estimate in a manner analogous to step-selection function using only other conspecifics as opposed to environmental variables as a covariate. Because both resources and populations were normalized to 1, the ratio between α and β can be interpreted as the relative importance of foraging to social cohesion. It does appear a certain balance between these two parameters is needed to successfully maintain, acquire, or adapt a migratory phenology.

Migration timing and location parameter can be similarly straightforwardly estimated from movement data (Cagnacci et al., 2015; Gurarie et al., 2019). Thus, for example, Gurarie et al. (2019) explicitly estimated the ranging area, timing, and seasonal range locations for migratory caribou (*Rangifer tarandus*), identifying the kind of inter-annual variation that is reflected in the stochastic scenarios explored here as well as some trends in the timing of migration. We note that our underlying assumption of the migration "urge" is consistent with the strong endogenous programs to migrate that are well-documented. Birds in particular exhibit a seasonal restlessness known as *Zugunruhe* (Berthold, 1999; Helm, 2006).

Individual based models have shown that collective knowledge is important, if not essential, to the evolution and process of migration (Shaw and Couzin, 2013; Guttal and Couzin, 2010; Berdahl et al., 2018). In our model, we assume that the migration process itself is driven by a collective trigger for the timing and locations of seasonal ranges and migration behavior. Synchrony of migration timing and high site fidelity are well documented for migratory species (Gurarie et al., 2019; Joly et al., 2021). We note, however, that diffusion-advection models can also be interpreted as a probabilistic description of a single individual's movement. In this case, λ would correspond to an individual home-range and β would be an individual's tendency to be drawn to the center of that home range, akin to an individual migratory Ornstein-Uhlenbeck process (Gurarie et al., 2017).

The reference memory parameter κ is, of course, impossible to observe directly. Our model does, however, allow us to explore in an heuristic way the conditions under which a strong cultural tendency to migrate with certain fixed patterns can help a population hedge against stochasticity (Abrahms et al., 2019; Fagan, 2019). An extremely conservative behavior may be the best way to hedge against stochasticity (high κ values in figure 7) as it serves no benefit to change behavior based on recent experiences if they do not inform what might happen in the future. However, this extreme conservatism is, by definition, incapable of adapting when there is a consistent shift in resource distribution (figure 8). In cases where both processes are occurring, we did, as predicted, see a slight improvement in adaptability when some long-term reference memory was used to stabilize the inclination to adapt, visible as peaks in figure 8 at κ values around 0.8.

Importantly, our model did not include any selection, inheritance or birth or death processes, i.e. there was no evolutionary maximization of a fitness, as in many models that explicitly explore the evolution of migration (e.g. Guttal and Couzin, 2010; Shaw and Couzin, 2013; Anderson et al., 2013). Nonetheless, it is instructive to compare the fundamental assumptions behind such evolutionary individual based models and a social memory based model like ours. For example, Anderson et al. (2013) explored the resilience of a population under selective pressure under persistent trends and

increased stochasticity of a drifting optimal resource window, showing that a certain amount of heritable phenotypic plasticity is necessary to adapt successfully to climate change even at the cost of efficiency. Our model underscores the fact that some level of resilience and adaptability can be attained with a purely cognitive process that balances sociality with long and short term collective memory. Importantly, this knowledge must be transmitted through social and cultural, rather than genetic, pathways. The high level of sociality among migratory animals, as well as multi-annual parent offspring bonds, are an evident pathway for that kind of transmission. As with those evolutionary models, however, it is clear that when changes are too rapid, no amount of cognition can help entirely mitigate against adverse outcomes. Furthermore, if behaviors are not sufficiently plastic (i.e., if κ is too close to 1), then adaptation is that much more difficult.

Rapid environmental change, both global warming and increased anthropogenic development, is causing severe and dramatic impacts to the widespread and generally successful strategy of seasonal migration for many taxa, and the fate of many animal migrations is a topic of increasing concern (Kauffman et al., 2021; Wilcove and Wikelski, 2008). The ability of animals to respond to these changes depends deeply on their behavioral plasticity and cognitive abilities. The importance of those abilities is in direct proportion to the difficulty in studying them directly. By quantitatively exploring the properties of a heuristic model that distill many of the main properties of wild populations in dynamic and seasonal environments, we hope to have identified some broad patterns that might guide further empirical exploration of the cognitive underpinnings of adaptability and resilience.

Diffusion-advection models have a long pedigree in animal movement modeling (Skellam, 1951; Turchin, 1998; Okubo and Levin, 2001). These models are grounded in the general idea that animal movements, somewhat like movements of physical particles, combine random (diffusive) components with directed (advective) components. While direct relationships between diffusion models and movement data are somewhat tenuous (Gurarie and Ovaskainen, 2011; Potts and Schlägel, 2020), as a theoretical tool for exploring processes they are invaluable for their versatility and the relative ease of numeric computation of the partial differential equations (PDEs) that describe them mathematically. Much theoretical and some applied work has been done on refining the basic assumptions of diffusion models, e.g. by including heterogeneity in populations (Skalski and Gilliam, 2003; Gurarie et al., 2009), fat-tailed dispersal kernels (Kot et al., 1996), non-linear or otherwise complex responses to resources and conspecifics. But perhaps the greatest difference between animals and randomly moving passive particles described by diffusion models is cognition, including social behavior and memory. Refinements to diffusion-advection equations have revealed conditions under which non-local information gathering (Fagan et al., 2017) and behavioral switching may confer foraging advantages (Fagan et al., 2019), in particular when resources are dynamic and patchy. While diffusion models that incorporate social movements (swarming, schooling, herds) have been well-studied (Okubo, 1986; Grünbaum, 1994; Mogilner and Edelstein-Keshet, 1999), the interacting role of memory and sociality in a specifically migratory framework has been relatively unexplored.

5 NOMENCLATURE

CONFLICT OF INTEREST STATEMENT

The authors declare that the research was conducted in the absence of any commercial or financial relationships that could be construed as a potential conflict of interest.

AUTHOR CONTRIBUTIONS

EG and WFF provided the original idea. EG and SP developed and ran models and analysis. All authors contributed to the writing.

FUNDING

EG, WFF, GCC and RSC, were supported in part by NSF award DMS 1853478. EG and WFF were further partially supported by NSF grant IIBR 1915347.

ACKNOWLEDGMENTS

The authors are grateful to Quentin Read at SESYNC for computational support and advice for multi-node multi-core model runs.

DATA AVAILABILITY STATEMENT

The only data analyzed in this manuscript was generated by simulation scripts made available in the GitHub repository at <https://github.com/EliGurarie/memorymigration>.

REFERENCES

- Abrahms, B., Hazen, E. L., Aikens, E. O., Savoca, M. S., Goldbogen, J. A., Bograd, S. J., et al. (2019). Memory and resource tracking drive blue whale migrations. *Proceedings of the National Academy of Sciences* 116, 5582–5587
- Anderson, J. J., Gurarie, E., Bracis, C., Burke, B. J., and Laidre, K. L. (2013). Modeling climate change impacts on phenology and population dynamics of migratory marine species. *Ecological Modelling* 264, 83–97
- Avgar, T., Street, G., and Fryxell, J. M. (2014). On the adaptive benefits of mammal migration. *Canadian Journal of Zoology* 92, 481–490. doi:10.1139/cjz-2013-0076
- Bauer, S., McNamara, J. M., and Barta, Z. (2020). Environmental variability, reliability of information and the timing of migration. *Proceedings of the Royal Society B: Biological Sciences* 287, 20200622. doi:10.1098/rspb.2020.0622
- Berdahl, A. M., Kao, A. B., Flack, A., Westley, P. A., Codling, E. A., Couzin, I. D., et al. (2018). Collective animal navigation and migratory culture: from theoretical models to empirical evidence. *Philosophical Transactions of the Royal Society B: Biological Sciences* 373, 20170009. doi:10.1098/rstb.2017.0009
- Berthold, P. (1999). A comprehensive theory for the evolution, control and adaptability of avian migration. *Ostrich* 70, 1–11. doi:10.1080/00306525.1999.9639744
- Bhattacharyya, A. (1943). On a measure of divergence between two statistical populations defined by their probability distributions. *Bull. Calcutta Math. Soc.* 35, 99–109
- Bischof, R., Loe, L. E., Meisingset, E. L., Zimmermann, B., Van Moorter, B., and Mysterud, A. (2012). A migratory northern ungulate in the pursuit of spring: jumping or surfing the green wave? *The American Naturalist* 180, 407–424
- Bracis, C. and Mueller, T. (2017). Memory, not just perception, plays an important role in terrestrial mammalian migration. *Proceedings of the Royal Society B: Biological Sciences* 284, 20170449
- Breiman, L. (2001). Random forests. *Machine learning* 45, 5–32
- Cagnacci, F., Focardi, S., Ghisla, A., van Moorter, B., Merrill, E. H., Gurarie, E., et al. (2015). How many routes lead to migration? comparison of methods to assess and characterize migratory movements. *Journal of Animal Ecology* 85, 54–68. doi:10.1111/1365-2656.12449

- Chapman, B. B., Brönmark, C., Nilsson, J.-Å., and Hansson, L.-A. (2011). The ecology and evolution of partial migration. *Oikos* 120, 1764–1775. doi:10.1111/j.1600-0706.2011.20131.x
- Dingle, H. (2014). *Migration: the biology of life on the move* (Oxford University Press, USA)
- Elzhov, T. V., Mullen, K. M., Spiess, A.-N., and Bolker, B. (2016). *minpack.lm: R Interface to the Levenberg-Marquardt Nonlinear Least-Squares Algorithm Found in MINPACK, Plus Support for Bounds*. R package version 1.2-1
- Fagan, W., Gurarie, E., Bewick, S., Howard, A., Cantrell, R., and Cosner, C. (2017). Perceptual ranges, information gathering, and foraging success in dynamic landscapes. *The American Naturalist* 189, 474–489. doi:10.1086/691099
- Fagan, W., Hoffman, T., Dahiya, D., Gurarie, E., Cantrell, R., and Cosner, C. (2019). Improved foraging by switching between diffusion and advection: benefits from movement that depends on spatial context. *Theoretical Ecology* 13, 127–136. doi:10.1007/s12080-019-00434-w
- Fagan, W. F. (2019). Migrating whales depend on memory to exploit reliable resources. *Proceedings of the National Academy of Sciences* 116, 5217–5219. doi:10.1073/pnas.1901803116
- Fagan, W. F., Cantrell, R. S., Cosner, C., Mueller, T., and Noble, A. E. (2011). Leadership, social learning, and the maintenance (or collapse) of migratory populations. *Theoretical Ecology* 5, 253–264. doi:10.1007/s12080-011-0124-2
- Fryxell, J. M., Greever, J., and Sinclair, A. (1988). Why are migratory ungulates so abundant? *The American Naturalist* 131, 781–798
- Grünbaum, D. (1994). Translating stochastic density-dependent individual behavior with sensory constraints to an eulerian model of animal swarming. *Journal of Mathematical Biology* 33, 139–161. doi:10.1007/BF00160177
- Gurarie, E., Anderson, J. J., and Zabel, R. W. (2009). Continuous models of population-level heterogeneity inform analysis of animal dispersal and migration. *Ecology* 90, 2233–2242
- Gurarie, E., Cagnacci, F., Peters, W., Fleming, C. H., Calabrese, J. M., Mueller, T., et al. (2017). A framework for modelling range shifts and migrations: asking when, whither, whether and will it return. *Journal of Animal Ecology* 86, 943–959
- Gurarie, E., Hebblewhite, M., Joly, K., Kelly, A. P., Adamczewski, J., Davidson, S. C., et al. (2019). Tactical departures and strategic arrivals: Divergent effects of climate and weather on caribou spring migrations. *Ecosphere* 10, e02971
- Gurarie, E. and Ovaskainen, O. (2011). Characteristic spatial and temporal scales unify models of animal movement. *The American Naturalist* 178, 113–123
- Guttal, V. and Couzin, I. D. (2010). Social interactions, information use, and the evolution of collective migration. *Proceedings of the National Academy of Sciences* 107, 16172–16177. doi:10.1073/pnas.1006874107
- Helm, B. (2006). Zugunruhe of migratory and non-migratory birds in a circannual context. *Journal of Avian Biology* 37, 533–540. doi:10.1111/j.2006.0908-8857.03947.x
- Jesmer, B. R., Merkle, J. A., Goheen, J. R., Aikens, E. O., Beck, J. L., Courtemanch, A. B., et al. (2018). Is ungulate migration culturally transmitted? Evidence of social learning from translocated animals. *Science* 361, 1023–1025
- Joly, K., Gurarie, E., Hansen, D. A., and Cameron, M. D. (2021). Seasonal patterns of spatial fidelity and temporal consistency in the distribution and movements of a migratory ungulate. *Ecology and Evolution* 11, 8183–8200. doi:10.1002/ece3.7650
- Kauffman, M. J., Cagnacci, F., Chamaillé-Jammes, S., Hebblewhite, M., Hopcraft, J. G. C., Merkle, J. A., et al. (2021). Mapping out a future for ungulate migrations. *Science* 372, 566–569.

- doi:10.1126/science.abf0998
- Kölzsch, A., Bauer, S., De Boer, R., Griffin, L., Cabot, D., Exo, K.-M., et al. (2015). Forecasting spring from afar? Timing of migration and predictability of phenology along different migration routes of an avian herbivore. *Journal of Animal Ecology* 84, 272–283
- Kot, M., Lewis, M. A., and Driessche, P. v. d. (1996). Dispersal data and the spread of invading organisms. *Ecology* 77, 2027–2042
- Lin, H.-Y., Fagan, W. F., and Jabin, P.-E. (2021). Memory-driven movement model for periodic migrations. *Journal of Theoretical Biology* 508, 110486. doi:10.1016/j.jtbi.2020.110486
- Merkle, J. A., Monteith, K. L., Aikens, E. O., Hayes, M. M., Hersey, K. R., Middleton, A. D., et al. (2016). Large herbivores surf waves of green-up during spring. *Proceedings of the Royal Society B: Biological Sciences* 283, 20160456. doi:10.1098/rspb.2016.0456
- Merkle, J. A., Sawyer, H., Monteith, K. L., Dwinnell, S. P. H., Fralick, G. L., and Kauffman, M. J. (2019). Spatial memory shapes migration and its benefits: evidence from a large herbivore. *Ecology Letters* 22, 1797–1805. doi:10.1111/ele.13362
- Mogilner, A. and Edelstein-Keshet, L. (1999). A non-local model for a swarm. *Journal of Mathematical Biology* 38, 534–570. doi:10.1007/s002850050158
- Okubo, A. (1986). Dynamical aspects of animal grouping: Swarms, schools, flocks, and herds. *Advances in Biophysics* 22, 1–94. doi:10.1016/0065-227X(86)90003-1
- Okubo, A. and Levin, S. (2001). *Diffusion and Ecological Problems: Modern Perspectives* (New York: Springer Verlag)
- Park, H., Jeong, S., and Peñuelas, J. (2020). Accelerated rate of vegetation green-up related to warming at northern high latitudes. *Global Change Biology* 26, 6190–6202. doi:10.1111/gcb.15322
- Potts, J. R. and Schlägel, U. E. (2020). Parametrizing diffusion-taxis equations from animal movement trajectories using step selection analysis. *Methods in Ecology and Evolution* 11, 1092–1105. doi:10.1111/2041-210X.13406
- Renner, S. S. and Zohner, C. M. (2018). Climate change and phenological mismatch in trophic interactions among plants, insects, and vertebrates. *Annual Review of Ecology, Evolution, and Systematics* 49, 165–182. doi:10.1146/annurev-ecolsys-110617-062535
- Robinson, R., Crick, H., Learmonth, J., Maclean, I., Thomas, C., Bairlein, F., et al. (2009). Travelling through a warming world: climate change and migratory species. *Endangered Species Research* 7, 87–99. doi:10.3354/esr00095
- Seebacher, F. and Post, E. (2015). Climate change impacts on animal migration. *Climate Change Responses* 2. doi:10.1186/s40665-015-0013-9
- Shaw, A. K. (2016). Drivers of animal migration and implications in changing environments. *Evolutionary Ecology* 30, 991–1007. doi:10.1007/s10682-016-9860-5
- Shaw, A. K. and Couzin, I. D. (2013). Migration or residency? the evolution of movement behavior and information usage in seasonal environments. *The American Naturalist* 181, 114–124
- Skalski, G. T. and Gilliam, J. F. (2003). A diffusion-based theory of organism dispersal in heterogeneous populations. *The American Naturalist* 161, 441–458
- Skellam, J. G. (1951). Random dispersal in theoretical populations. *Biometrika* 38, 196–218
- Soetaert, K. and Meysman, F. (2012). Reactive transport in aquatic ecosystems: Rapid model prototyping in the open source software r. *Environmental Modelling and Software* 32, 49–60
- Soetaert, K., Petzoldt, T., and Setzer, R. W. (2010). Solving differential equations in R: Package deSolve. *Journal of Statistical Software* 33, 1–25. doi:10.18637/jss.v033.i09

- 559 Turchin, P. (1998). *Quantitative analysis of movement: measuring and modeling population*
560 *redistribution in animals and plants* (Sinauer Associates)
- 561 Wilcove, D. S. and Wikelski, M. (2008). Going, going, gone: Is animal migration disappearing.
562 *PLoS Biology* 6, e188. doi:10.1371/journal.pbio.0060188
- 563 Xu, W., Barker, K., Shawler, A., Scoyoc, A. V., Smith, J. A., Mueller, T., et al. (2021). The
564 plasticity of ungulate migration in a changing world. *Ecology* 102. doi:10.1002/ecy.3293

1 SUPPLEMENTARY MATERIAL

1.1 Drifting resource

The drifting resource function has the following properties

1. The total amount of resource across space is constant throughout the year.
2. At the beginning, middle, and end of the year the resource is uniformly distributed.
3. At some peak time $\mu_t < \tau/2$, the resource concentrates at a location $\mu_x < \chi$ with a spatial deviation σ_x and a temporal deviation σ_t (where τ is the length of the year and χ is the extent of the spatial domain).
4. The resource peaks exactly symmetrically at time $\tau - \mu_t$ and location $-\mu_x$ with the same variances.

To generate a resource with these properties, we distributing the resource in space as a beta distribution, where the two shape and scale parameters vary sinusoidally in such a way as to fulfill the criteria above. Thus:

$$h(x, t, \theta) = \chi B(x/\chi, a(t, \theta), b(t, \theta))$$

where χ is the maximum value (domain) of x , $B(x, a, b)$ is the beta distribution, θ represents the set of parameters $t_r, x_r, \sigma_t, \sigma_x$, and the two shape parameters are given by:

$$a(t) = \frac{m}{s^2}(s^2 + m - m^2)$$

$$b(t, x', \sigma') = (m - 1) \left(1 + \frac{m}{s}(m - 1) \right)$$

where $m(t)$ and $s(t)$ describe the dynamic mean and variance of the resource peak. These equations are solutions to the mean and variance of the beta distribution, $\mu = \alpha/(\alpha + \beta)$, $\sigma^2 = \frac{\alpha\beta}{(\alpha + \beta)^2(\alpha + \beta + 1)}$.

The means and variances themselves are Gaussian pulses, with the mean peaking at μ_x at time μ_t with standard deviation σ_t and at $-\mu_x$ at time $\tau - \mu_t$ and the standard deviation pulsing from $2\chi/\sqrt{12}$ (corresponding to a uniform distribution over the domain $-\chi$ to χ) at times 0, $\tau/2$ and τ down to σ_x at t_r and $\tau - t_r$, with standard deviation (in time) σ_t .